Dehydroindigo, the Forgotten Indigo and Its Contribution to the Color of Maya Blue

ARTICLE *in* THE JOURNAL OF PHYSICAL CHEMISTRY A · FEBRUARY 2010

Impact Factor: 2.69 · DOI: 10.1021/jp907718k · Source: PubMed

Dehydroindigo, the Forgotten Indigo and Its Contribution to the Color of Maya Blue

Raquel Rondão,[†] J. Sérgio Seixas de Melo,*[,†] Vasco D. B. Bonifácio,[‡] and Maria J. Melo[‡,§]

Department of Chemistry, University of Coimbra, 3004-535 Coimbra, Portugal, REQUIMTE-CQFB and Faculty of Sciences and Technology of the New University of Lisbon, Campus da Caparica, Portugal, and Department of Conservation and Restoration, New University of Lisbon, Campus da Caparica, Portugal

Received: August 10, 2009; Revised Manuscript Received: October 19, 2009

A comprehensive investigation of the electronic spectral and photophysical properties of the oxidized form of indigo, dehydroindigo (DHI), has been carried out in solution at 293 K. It is shown that dehydroindigo readily converts into its neutral keto form, the blue indigo, in a process which depends on the solvent and water content of the medium. DHI was investigated in toluene, in benzene, and in methanol and it was found that both the oxidized and the keto indigo forms are present in solution. In marked contrast to what has been found for keto-indigo, where the internal conversion channel dominates >99% of the excited state deactivation, or with the fully reduced leuco-indigo, where fluorescence, internal conversion, and singlet-to-triplet intersystem crossing coexist, in the case of DHI in toluene and benzene, the dominant excited state deactivation channel involves the triplet state. Triplet state yields (ϕ_T) of 70−80%, with negligible fluorescence (≤0.01%) are observed in these solvents. In methanol the ϕ_T value decreases to ∼15%, with an increase of the fluorescence quantum yield to 2%, which makes these processes competitive with the $S_1 \rightsquigarrow S_0$ internal conversion deactivation process. The data are experimentally compatible with the existence of a lowest lying singlet excited state of n,π^* origin in toluene and of π,π^* origin in methanol. A time-resolved investigation in the picosecond time domain suggests that the emission of DHI involves three interconnected species (involving rotational isomerism), with relative contributions depending on the emission wavelength. DFT calculations (B3LYP 6-31G** level) were performed in order to characterize the electronic ground (S_0) and excited singlet (S_1) and triplet (T_1) states of DHI. The HOMO−LUMO transition was found to accompany an $n \rightarrow \pi^*$ transition of the oxygen nonbonding orbitals to the central CC and adjacent C−N bonds. Calculations also revealed that in S_0 the two indole-like moieties deviate from planarity from ca. 20°, whereas in S_1 and T_1 the predicted structure is basically planar; a gradual decrease of the carbon−carbon central bond distance is seen in the order S_0, S_1, T_1. An additional study on the blue pigment Maya Blue was made, and the comparison between the solid-state spectra of indigo, DHI, and Maya Blue suggests that, in line with recent investigations, DHI is present together with indigo in Maya Blue. These results are relevant to the discussion of the involvement of dehydroindigo in the palette of colors of the ancient Maya Blue pigment.

Introduction

Indigo, a molecule which has influenced mankind's history for several millennia and is a chemical icon, still harbors mysteries. Indigo was the blue color used by almost all the ancient civilizations and one of the first natural molecules to be synthesized, thus paving the way to the modern chemical industry.[1] The blue indigo is a mythical molecule not only due to its magnificent color but also because of its remarkable stability as a dye and paint. Its presence (even until our days) in denim jeans preserves the identity and importance of this molecule. Relevant aspects of indigo's chemistry are related to the stability of this molecule as a dye. Its photodegradation was recently investigated, and it was shown that its reduced form, the leuco form, is significantly more prone to degradation than its neutral keto form.[2]

Dehydroindigo (DHI), the oxidized (and third) form of the blue indigo, has been the forgotten form of indigo. This may be related to its more limited stability and the fact that the more common leuco is the water-soluble form used in the dyeing processes, which when exposed to oxygen leads to the colored neutral keto form.

Nevertheless, although not normally isolated, DHI has gained recent interest since it was identified in the procedure leading to Maya Blue,[3−6] the source of blue of this ancient civilization, considered as the first fabricated organic (indigo)−inorganic (clay) hybrid.[7−9] Its chemical structure, although puzzling until recently, seems to involve the incorporation of indigo into palygorskite or sepiolite clays.[10−12] Recent works suggest that indigo reveals a strong attachment to this clays and that, together with DHI, it penetrates more deeply (and is consequently more protected) into the channels of palygorskite.[13] This incorporation protects the organic dye, leading to outstanding stability which has made possible the preservation of the color for centuries in paintings subjected to severe environment conditions, in particular those involving light (photodegradation). However, the mechanism leading to indigo's incorporation and its localization within the clay, i.e., if it is distributed in the surface or if it goes into the clay channels, or a distribution of these two, is still under debate.[13−16] It appears improbable that the blue indigo with its rigid structure can penetrate in its normal form into the palygorskite clay. Dehydroindigo and leuco-indigo seem more

* To whom correspondence should be addressed: e-mail, sseixas@ci.uc.pt; fax, 00351 239 827703.
[†] Department of Chemistry, University of Coimbra.
[‡] REQUIMTE-CQFB and Faculty of Sciences and Technology of the New University of Lisbon.
[§] Department of Conservation and Restoration, New University of Lisbon.

10.1021/jp907718k
Published on Web 01/07/2010

plausible forms for indigo to enter into the clay structure, since both these structures lack double bond character in the central bond connecting the two indole-like structures, making them more flexible and more likely to penetrate into the clay channels. Others have argued against this since indigo is found at the entrance of the clay channels.[14] However, whether it is keto, leuco, or dehydroindigo (or even the three) which are preferentially involved in the formation of Maya Blue is not the topic of the present work.

Instead, a comprehensive investigation was undertaken of the electronic spectral and photophysical properties of DHI in solution. This aims to provide new insights on this molecule, both on its own and also for potential interpretations of the origin of the color of the Maya civilization blue pigment, where it was found that DHI may play a substantial role.[6]

Experimental Section

Indigo was purchased from Aldrich. Dehydroindigo was synthesized by oxidation of indigo with calcium hydroxide and bromine, using a synthetic procedure reported elsewhere.[17] A purple solid was obtained after recrystallization from benzene.[18,19] The compound was found to readily convert into keto-indigo on alumina or silica chromatographic plates, and a complete purification of this dye by chromatography was found impracticable. In the IR spectrum no NH band was found and a strong band at 1726 cm^{-1} was observed, which is in accordance with reported data.[18,19]

The ^1H and ^{13}C NMR spectra were recorded on a Bruker ARX 400-spectrometer. Chemical shifts (δ) are reported in parts per million (ppm) using residual solvents protons as internal standards. The coupling constants are reported in hertz (Hz). Splitting patterns are designated as s (singlet), d (doublet), t (triplet), q (quartet), bs (broad singlet), m (multiplet), and bm (broad multiplet). ^1H NMR (400.1 MHz, $CDCl_3$) δ: 7.76−7.64 (8H, m). ^{13}C NMR (100.6 MHz, $CDCl_3$) δ: 189.50 (C-3), 159.52 (C-2), 155.22 (C-3a), 139.10 (C-7a), 136.79 (C-6), 130.36 (C-4), 125.06 (C-5), 124.42 (C-7).

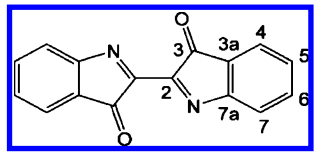

The solvents used were of spectroscopic or equivalent grade and were purified by conventional methods until no detectable fluorescence of the solvent could be seen at the excitation wavelengths used. Toluene and benzene were used as solvents for this study since they solubilize DHI and can be efficiently dried. Methanol was also used and was dried before using with P_2O_5 under an inert atmosphere. In nonpolar solvents such as cyclohexane or hexane, dehydroindigo shows a very poor solubility. Moreover the synthesis of DHI (from indigo) may not be 100% complete suggesting that some indigo may be present, even if in vestigial amounts.

Absorption and fluorescence spectra were recorded on Shimadzu UV-2100 and Horiba-Jobin-Ivon Spex Fluorog 3-22 spectrometers, respectively. Phosphorescence measurements were made in glasses at 77 K and used the same Spex Fluorog 3-22 spectrometer, equipped with a 1934 D phosphorimeter. The phosphorescence quantum yield was determined using benzophenone in ethanol ($\phi_{ph} = 0.84$) as a standard.[20] All of the fluorescence and phosphorescence spectra were corrected for the wavelength response of the system. The fluorescence quantum yields were measured using as standards quinquethiophene ($\phi_F = 0.36$ in dioxane)[21] and indigo in DMF ($\phi_F = 0.0023$).[22]

Singlet oxygen quantum yields measurements were performed on a Horiba-Jobin-Ivon SPEX Fluorog 3-22 using the Hamamatsu R5509-42 photomultiplier. For that, the use of a Schott RG1000 filter was essential to eliminate from the infrared signal all of the first harmonic contribution of the sensitizer emission in the region below 850 nm. The sensitized phosphorescence emission spectra of singlet oxygen from optically matched solutions of the samples and that of reference were obtained under identical experimental conditions. The singlet oxygen formation quantum yield was then determined by comparing the integrated area under the sensitized emission spectra of singlet oxygen of the samples solutions ($\int I(\lambda)^{compound} d\lambda$) and that of the reference solution ($\int I(\lambda)^{ref} d\lambda$) using eq 1.

$$\phi_\Delta^{compound} = \frac{\int I(\lambda)^{compound} d\lambda}{\int I(\lambda)^{ref} d\lambda} \phi_\Delta^{ref} \quad (1)$$

with ϕ_Δ^{ref} the singlet oxygen formation quantum yield of the reference compound. 1*H*-Phenalen-1-one in toluene ($\phi_\Delta = 0.93$) was used as standard.[23]

The fluorescence decays of the compounds were obtained with picosecond resolution with equipment described elsewhere[24] and were analyzed using the method of modulating functions implemented by Striker.[25] The experimental excitation pulse (fwhm = 21 ps) was measured using a LUDOX scattering solution in water. After deconvolution of the experimental signal, the time resolution of the apparatus is ca. 2 ps.

The experimental setup used to obtain triplet state absorption spectra and quantum yields involves an Applied Photophysics laser flash photolysis apparatus pumped by a Nd:YAG laser (Spectra Physics), as described in detail elsewhere.[26] Transient spectra were obtained by monitoring the optical density change at intervals of 10 nm over the 250−800 nm range and averaging at least 10 decays at each wavelength. First-order kinetics were observed for the decay of the lowest triplet state. Excitation was at 355 nm with an unfocused beam. Special care was taken in determining triplet yields to have optically matched dilute solutions (abs $\approx$ 0.2 in a 10 mm square cell) and low laser energy (2 mJ) to avoid multiphoton and triplet−triplet (T−T) annihilation effects. The triplet molar absorption coefficients were determined by the energy transfer method,[27] using pyrene, $\varepsilon_T = 20900\ M^{-1}\ cm^{-1}$ (420 nm, toluene and benzene) or $\varepsilon_T = 30400\ M^{-1}\ cm^{-1}$ (412 nm, methanol) depending on the solvent,[20] as triplet energy donor. The concentration of dehydroindigo was 10^{-5} M, and it was dissolved in toluene, benzene, or methanol solutions of pyrene 10^{-2} M. Before experiments, all solutions were degassed with argon for ≈20 min and sealed. The triplet−triplet molar absorption coefficients were then determined from eq 2

$$\frac{\varepsilon_{TT}^D}{\varepsilon_{TT}^A} = \frac{\Delta OD^D}{\Delta OD^A} \quad (2)$$

where ε_{TT}^D and ε_{TT}^A are the triplet molar absorption coefficients of donor and acceptor, respectively; ΔOD^D is the maximum absorbance from the transient triplet−triplet absorption spectra of the donor in the absence of acceptor; ΔOD^A is the maximum absorbance of the acceptor triplet when both the donor and the acceptor are present. When the acceptor decay rate constant (k_3) is not negligible, corrections were made for determination of ΔOD^A using eq 3

$$\Delta OD^{A}_{obs} = \Delta OD^{A} \exp\left[-\frac{\ln k_2/k_3}{k_2/k_3 - 1}\right] \quad (3)$$

where k_2 is the donor decay rate constant in the presence of acceptor and ΔOD^{A}_{obs} is taken from the maximum observed in the triplet−singlet difference spectra of the acceptor in the presence of donor.

The intersystem-crossing yields for the compounds (ϕ_T^{cp}) were obtained by comparing the ΔOD at 530 nm of benzene solutions of benzophenone (standard) optically matched (at the laser excitation wavelength) and of the compound using eq 4

$$\phi_T^{cp} = \frac{\varepsilon_{TT}^{benzophenone}}{\varepsilon_{TT}^{cp}} \frac{\Delta OD_{max}^{cp}}{\Delta OD_{max}^{benzophenone}} \phi_T^{benzophenone} \quad (4)$$

The ground-state geometry was optimized using the density functional theory (DFT) by means of the Gaussian 03 program,[28] employing the Becke's hybrid three parameter exchange functional (B3) combined with the nonlocal correlation functional of Lee, Yang, and Parr (LYP)[29] and with the 6-31G** Gaussian atomic basic states.[30] Molecular orbital contours were plotted using Molekel 5.3.[31] The excited state parameters were obtained either from the electron promotion from the HOMO to LUMO orbitals (vertical transitions) or from the energies of the optimized structures (adiabatic).

Maya Blue was produced by mixing 2 g of sepiolite (Tolsa, Pangel S9) with 0.1 g of indigo (5% w/w) in 30 mL of water. The mixture was then stirred for 1 h and further heated, for 5 h, at 190 °C. The obtained solid was rinsed with distilled water and acetone until no trace of indigo (as followed by the absorption spectra) could be found in the washing solvent. The final step consisted in the acid attack (with concentrated nitric acid), followed by rinsing again with distilled water and acetone; again no traces of indigo could be found in the washing solvent(s). The obtained pigment was then left drying at room temperature.

Maya Blue from Kremer Pigmente GmbH & Co. KG was also used, but since there is no indication of the clay used, we have made our studies with the Maya Blue synthesized in our laboratories.

The solid-state spectra were recorded on a Shimadzu UV-2450 by diffuse reflection using an integrating sphere model reference ISR-2200. The samples for the solid-state spectra were obtained by mixing the different pigments (Maya Blue, indigo and DHI) with barium sulfate. Before spectra of the solid sample were run, a baseline, with barium sulfate, was obtained.

Results and Discussion

Although indigo takes up hydrogen on conversion into leuco-indigo (Scheme 1), and more energetic reduction even breaks the double bond,[2] it can also be dehydrogenated by the reaction given in Scheme 1. The oxidation or reduction of indigo depends on the solvent media. In the case of reduction to the leuco form, the formation of a highly reducing media (usually sodium dithionate in alkaline solution) is needed, whereas oxidation, with formation of dehydroindigo, is made with a strongly oxidizing reagent (bromine was used in the present experiments; see Experimental Section). The dehydroindigo which is thus formed is much more soluble than indigo itself in most organic solvents. It is very easily hydrogenated back to indigo in the manner shown in Scheme 1 (read from right to left) by even vestigial amounts of water. This, in reality, poses a challenge to characterize the "pure" DHI in solution. Indeed, in the present study we were unable to obtain DHI completely free of indigo.

SCHEME 1: Interconversion between the Neutral Indigo and Its Oxidized Form: Dehydroindigo

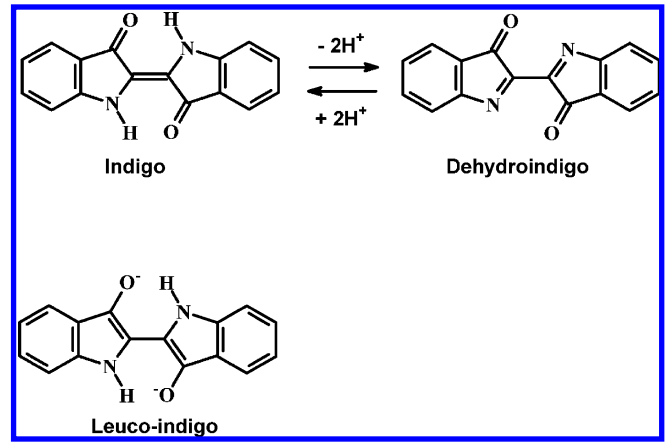

Nevertheless since they absorb and emit in different spectral regions, it was possible to make a detailed spectral and photophysical investigation of DHI in solution.

Absorption and Emission. DHI absorbs in the visible region, with wavelength maxima (λ_{max}) at 455 nm (toluene) and 400 nm (methanol), displaying an orange-brown color both in the solid state and in liquid solution. It is worth noting that dehydroindigo clearly presents different absorption (and emission) maxima and photophysical parameters depending on the solvent. As will be shown below, this compound is highly sensitive to the polarity and particularly to the water content of the media.

The absorption spectrum of DHI in toluene displays two bands in the visible region with λ_{max} = 455 and 600 nm; see Figure 1. These are attributed to the oxidized form of indigo, dehydroindigo, and to the neutral (keto) blue indigo, respectively. The longer wavelength absorption band, associated with indigo, has its origin in the incomplete conversion (from the synthetic procedure) of the latter into dehydroindigo or to a (residual) formation of indigo (from dehydroindigo) by hydrogen abstraction (Scheme 1) of the solvent; this occurs even though the solvent has been dried to exhaustion.

In this same Figure 1, the evolution with time of the absorption spectra of DHI in nondried toluene is also presented. The conversion of DHI into indigo is clear with the 600 nm band (indigo) increasing at the expense of the decrease of the 455 nm (DHI) band, with a clear isosbestic point at 531 nm.

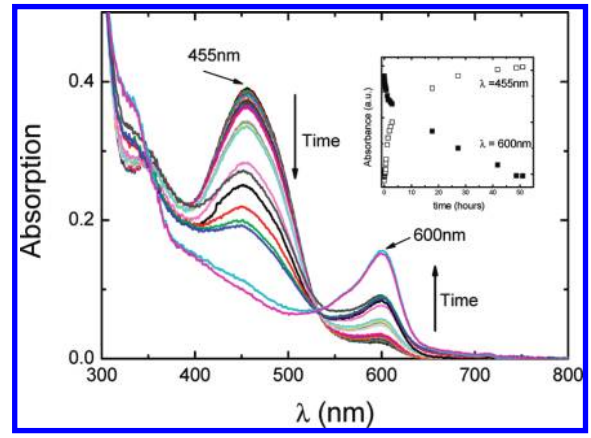

Figure 1. Dehydroindigo absorption spectra variation with time, in nondried toluene at T = 293 K. Show as inset plot is the dependence with time of the absorption maxima of DHI and indigo.

TABLE 1: Spectral (Absorption and Emission Wavelength Maxima and Singlet and Triplet Extinction Coefficients) and Photophysical (Fluorescence Quantum Yield, Singlet Oxygen Quantum Yield, Phosphorescence Quantum Yield, and Triplet Formation Quantum Yield) Parameters for Dehydroindigo in Several Solvents at $T = 293$ K

	λ_{abs}^{max}	ε_{ss}	λ_{fluo}^{max}		ϕ_F[b]		ϕ_Δ	ϕ_{Ph}	ϕ_T	ε_{TT}
solvent	(nm)	(M^{-1} cm^{-1})	(nm)[a]							(M^{-1} cm^{-1})
toluene	455, 600	4870 ± 150	544, 645 ($\lambda_x = 455$ nm)	636 ($\lambda_x = 600$ nm)	0.00032 (±0.00003) ($\lambda_x = 455$ nm)	0.0012 (±0.0001) ($\lambda_x = 600$ nm)	0.60 (±0.01)	N.D.[c]	0.71 (±0.05)	10240 (±400)
benzene	456, 600	5056 ± 90	541, 645 ($\lambda_x = 457$ nm)	635 ($\lambda_x = 600$ nm)	0.000081 (±0.000004) ($\lambda_x = 457$ nm)	0.0010 (±0.00005) ($\lambda_x = 600$ nm)	0.83 (±0.07)	N.D.[c]	0.83 (±0.08)	10947 (±108)
methanol	400, 607	3005 ± 68	535 ($\lambda_x = 400$ nm)	672 ($\lambda_x = 606$ nm)	0.0250 (±0.0003) ($\lambda_x = 400$ nm)	0.0011 (±0.0001) ($\lambda_x = 607$ nm)	0.15 (±0.01)	0.159 (±0.013)	0.156 (±0.014)	8975 (±375)

[a] The wavelength maxima of the bands were obtained with the excitation wavelength (λ_x) indicated. [b] The fluorescence quantum yields were obtained from the integrated bands which were obtained with the excitation wavelength (λ_x) indicated. [c] ND, not determined.

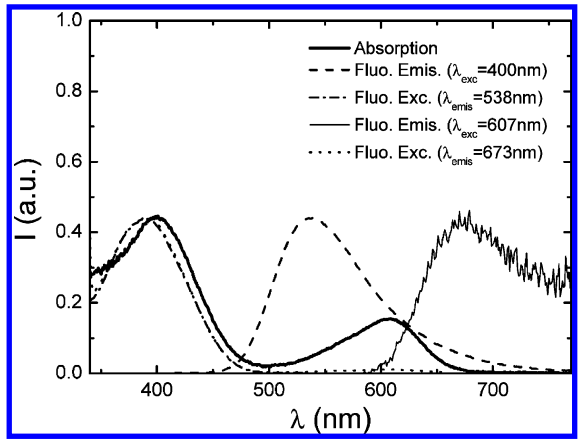

Figure 2. Absorption, fluorescence emission, and excitation spectra (normalized) for dehydroindigo in methanol, at $T = 293$ K.

From the inset plot, where the dependence, with time, of the absorption values at 600 nm (indigo) and 455 nm (DHI) is presented, it can be seen that the formation of indigo is concomitant with the decrease of DHI and that after ~40 h the formation of indigo at the expenses of DHI is (essentially) complete, with the final coexistence of the two forms (neutral and oxidized) in solution. In contrast, with dried toluene the presence of the two bands (DHI and indigo) is observed but there is effectively no change (evolution) of the spectra with time.

In toluene (and benzene) the emission spectrum of DHI was found to depend of the excitation wavelength. When excitation is made at 455 nm (dehydroindigo) the emission spectra show two bands with maxima (λ_{em}) at ~540 nm and ~645 nm (figure not shown); see Table 1. However, when excitation is at 600 nm (indigo absorption band) a single band is observed with a wavelength emission maxima, λ_{em}, at 640 nm.[22] These results support the coexistence of dehydroindigo and indigo in the emission spectra and that when excitation is made in the absorption region of DHI, two bands are observed (indigo and DHI), whereas when the excitation is made in the absorption band of indigo, where dehydroindigo does not absorb, the resultant emission is solely from indigo. Similar behavior was found for DHI in benzene solution.

In methanol, DHI displays different spectral behavior from that observed in toluene, Figure 2. In addition to the indigo absorption band (shifted to $\lambda_{max} = 607$ nm, Table 1), the 455 nm band, previously observed in toluene/benzene, is now blue-shifted to 400 nm. Moreover, when excitation is made in this band, the emission of DHI is now only 5 nm blue-shifted, $\lambda_{max} = 535$ nm, relative to toluene. In addition, the fluorescence quantum yields in methanol increase by ca. 1 order of magnitude compared with those in toluene (or benzene); see Table 1.

In methanol (Figure 2) as with toluene and benzene solutions, excitation at the longest wavelength band of DHI leads to emission from indigo.

These conclusions were further validated from the excitation spectra observed at the dehydroindigo and indigo emission bands, which reproduced the bands of the absorption spectra of these two species. A small shift was observed between the absorption and excitation bands of DHI (Figure 2). However, this difference is due to the fact that with the absorption, the spectrum of DHI overlaps that of indigo, leading to the small shift in the band, which is not observed in the excitation spectrum since it reproduces the "absorption" of the "pure" DHI.

In molecules where the lowest lying singlet states are of n,π^* and π,π^* origin, hydrogen bonding can be established between the nitrogen or oxygen (in the present case in the C═O group) atoms and the solvent molecules, resulting in a stabilization of the n,π^* and inversion of the lowest lying neighboring n,π^* and π,π^* states.[32] In toluene, the water molecules are available to promote an efficient hydrogen bonding with the lone pair electrons of the oxygen in the carbonyl groups of DHI. This, consequently, leads to a stabilization of the n,π^* state (relative to the π,π^*) by decreasing the energy of the nonbonding orbitals further resulting in a poor fluorescence emission (low ϕ_F in Table 1), which is also a way of identification of an n,π^* state.[32] In contrast, when methanol is the solvent, the hydrogen-bond ability of this solvent is not so efficient (as compared with water) and consequently there is a poorer stabilization of the n,π^* state, and now the lowest lying state is of π,π^* origin. Indeed, in Table 1 the photophysical parameter ϕ_F (see below further discussion) is much lower in toluene than it is in methanol. Also the location of the 400 nm band in toluene (which is blue-shifted relative to methanol) implies that this is an S_2 of π,π^* origin whereas the n,π^* transition is buried underneath this intense band. These observations are also in agreement with the molecular orbital contours obtained by TDDFT calculations; see discussion below.

Other relevant findings relative to DHI can be seen in the photophysical parameters in Table 1. In marked contrast with keto-indigo, where the main deactivation channel of the excited state is the radiationless internal conversion,[22,33,34] or with leuco-indigo, where fluorescence, internal conversion, and intersystem crossing coexist,[22] with DHI in toluene and benzene, triplet state formation is now the main deactivation route for the first singlet excited state. In methanol, although the ϕ_T value decreases to 0.156, this is still significantly higher than the value of the keto form, the blue indigo ($\phi_T = 0.0068$[34]). This has implications on the nature of the process leading to the deactivation of indigo's excited state. Indeed intramolecular proton transfer, between the N—H and C═O of indigo, was proposed to be responsible for the high efficiency of the internal conversion

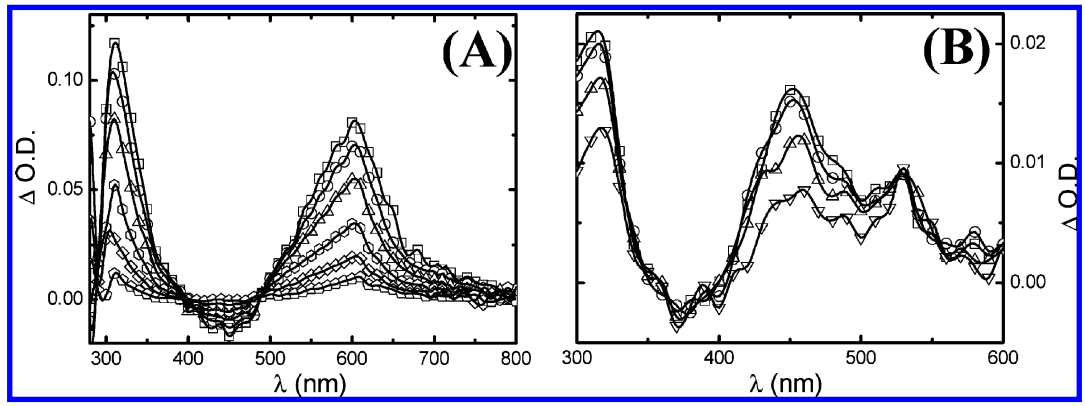

Figure 3. Transient triplet−triplet absorption spectra obtained for dehydroindigo in toluene (A) and methanol (B), obtained with different delay times after laser flash, $T = 293$ K.

deactivation route.[33,35] Methylation of the N−H groups (N−CH_3) has shown the additional possibility of rotational isomerization to indigo's excited state which competes with the other deactivation pathways.[36,37] Blocking the possibility of rotation around the double bond was investigated with an indigo derivative, where fluorescence and intersystem crossing were found to dominate the deactivation of the excited state of this molecule.[35] However, with the oxidized form, dehydroindigo, intramolecular proton transfer is precluded, and intersystem crossing is now an important pathway for the excited state deactivation in comparison with indigo, thus providing conclusive evidence that the N−H groups (presumably through proton transfer to C═O) have a crucial role in the excited-state deactivation (and hence photostability) of indigo.

Triplet State and Singlet Oxygen Sensitization. The transient triplet−triplet difference absorption spectrum of dehydroindigo in toluene (which is identical to the spectra in benzene) is depicted in Figure 3A. A strong absorption at 605 nm with depletion at 450 nm is observed; see also Table 1. The decay traces in the depletion and maxima regions are identical, thus showing that the ground state is recovered at the expense of the transient triplet generated. In methanol (Figure 3B), the transient triplet−triplet spectra show a depletion band at 400 nm, consistent with the absorption spectra, Figure 2, with a maximum at 450 nm; see Table 1.

In the case of the nonprotic solvents benzene and toluene, the intense transient signals are also mirrored in the high intersystem crossing values obtained (see Table 1).

Singlet oxygen was sensitized by DHI, and the respective quantum yields were obtained in the three solvents: toluene, benzene, and methanol, Table 1. In the cases where the oxidized species (dehydroindigo) is dominant, the values are high, thus showing that the triplet state efficiently transfers energy to molecular oxygen. In the case of methanol, the ϕ_Δ values are smaller but still in agreement with the values obtained for ϕ_T; see Table 1. This behavior is similar to what is seen with other systems with π,π^* triplet states[34,38] (which is the case of DHI, see below) where the efficiency of singlet oxygen production from the triplet state is high, $S_\Delta \sim 1$, which is not necessarily always true when the triplet state is of n, π^* origin.[39]

Phosphorescence in Methanol. The phosphorescence emission spectrum of DHI was obtained in a rigid glass of methanol, Figure 4. It is worth noting that although the neutral keto-indigo does not phosphoresce, phosphorescence emission of leuco-indigo was previously observed for indigocarmine in methanol.[22] With the phosphorescence of DHI, we have observed emission maxima of 540 nm, a quantum yield of 0.159 (see Table 1), and a lifetime ~190 ms, which are characteristic parameters of

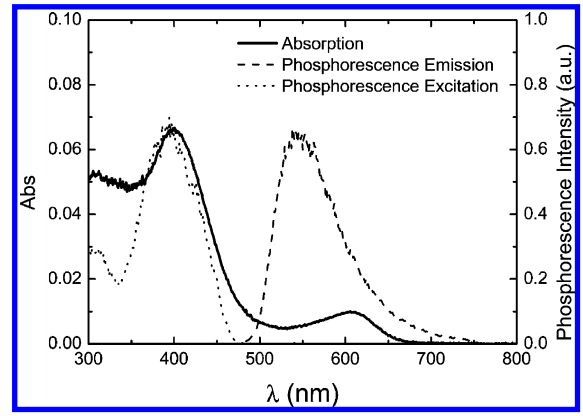

Figure 4. Absorption, phosphorescence emission, and excitation spectra (normalized) for dehydroindigo in methanol, at $T = 77$ K.

a triplet of π,π^* origin, similarly to what was found for keto-indigo.[34] The close relation between the ϕ_T and ϕ_{Ph} values shows that, in methanol, the triplet state mainly deactivates radiatively.

Time-Resolved Fluorescence Behavior. The fluorescence decays of dehydroindigo were obtained in methanol and glycerol and are presented in Figures 5 and 6, respectively. The decays are clearly dependent on the emission wavelength; see Figures 5 and 6.

The decays were collected with a time resolution of ≈3 ps[24] and could be fitted with triexponential decay laws according to eq 5

$$I_\lambda(t) = \sum_{ij} a_i e^{-t/\tau_j} \qquad (5)$$

where $I_\lambda(t)$ is the fluorescence intensity at the emission wavelength λ, a_j (with $i = 1, 2, 3, ...$) are the pre-exponential factors and τ_i ($j = 1, 2, 3$) the decay times; see Figure 5 and 6.

This is a priori unusual behavior since one would expect DHI singlet state to decay monoexponentially. A possible explanation of the three exponential nature of the decays involving (rotational) isomerization is as follows. The instantaneously excited DHI decays with 10−20 ps. This can, however, further convert in the excited state into two other structures/conformers of DHI (with different angles between the two isatin-like moieties, Scheme 2); on the basis of these data, the presence of some of these species/conformers in the ground state cannot be completely ruled out. With excitation at 425 nm, these two conformers emit with decay times of 680 ps and ~2 ns. This is again illustrated in Scheme 2. The rising component (negative pre-exponential factor) associated to the shorter component shows that this species gives rise, in the excited state, to the

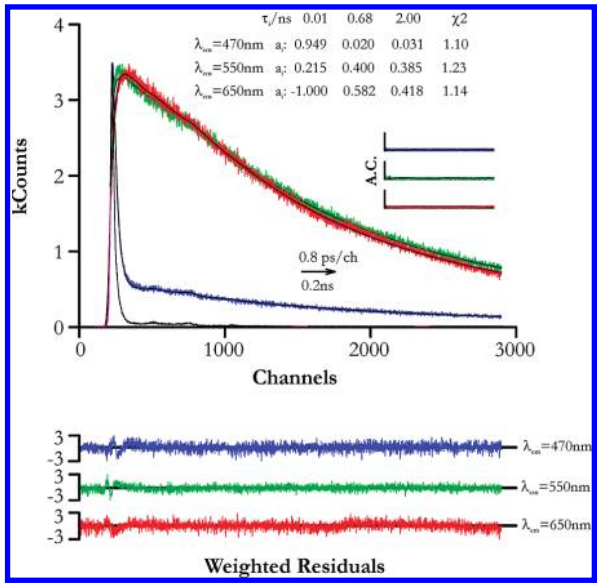

Figure 5. Fluorescence decays of dehydroindigo in methanol, at $T =$ 293 K, with excitation at 425 nm and collected at 470, 550, and 650 nm. Shown as insets are the decay times (τ/ns), pre-exponential factors (a_i), and chi-squared values (χ^2). Also shown are the weighted residuals for a better judgment of the quality of the fits. The black line is the pulse instrumental response.

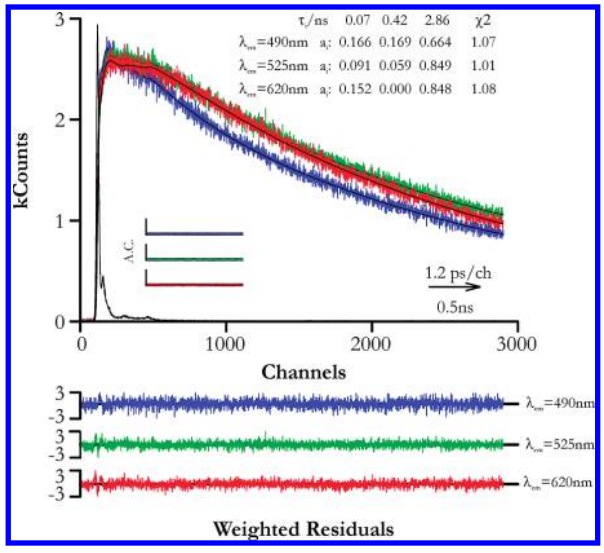

Figure 6. Fluorescence decays of dehydroindigo in glycerol, at $T =$ 253 K, with excitation at 425 nm and emission collected at 490, 525, and 620 nm. Shown as insets are the decay times (τ/ps), pre-exponential factors (a_i), and chi-squared values (χ^2). Also shown are the weighted residuals for a better judgment of the quality of the fits. The black line is the pulse instrumental response.

two other species with longer decay components and that this process most likely involves a rotation around the central C−C bond connecting the two isatin-like moieties. Since the model compound, isatin, is known to be nonfluorescent[40] (and this was also verified in this work), this means that none of the conformers involves a total conjugation rupture (decoupling) between the two (isatin-like) moieties.

It is worth remembering, once more, that the excitation spectra collected all over the emission spectra of DHI overlaps with the absorption of this compound. This indicates that the DHI conformers absorb in the same spectral region, with very similar absorption maxima; i.e., they are within the homogeneous broadening of these bands.

A further analysis of the possible involvement of rotational isomerism comes from changing the viscosity of the solvent. Although poorly soluble in several solvents, DHI was found to be soluble in glycerol (a highly viscous solvent, η (20 °C) = 1412 cP). At low temperature, −20 °C (Figure 6), the decays are, as with methanol, dependent on the emission wavelength. However, now the decay times have larger values than those found in methanol, but more significantly, the negative pre-exponential factor is now absent. This shows that the conversion of one conformer into the other (involving a rotational process) is precluded (at least in the excited state) and that the contribution of the different conformers comes from their relative proportions in the ground state. This is again given pictorially in Scheme 2. A more detailed investigation of the time-resolved behavior of DHI is currently under investigation.

The overall spectral and photophysical data obtained for DHI can be summarized in the diagram in Scheme 3, which can be further compared with that of indigo.[34,41] The first clear difference lies in the fact that the single bond character between the two isatin-like moieties in DHI breaks up the H-chromophore[18,42] character of indigo leading to a difference of 0.67 eV between the S_1-S_0 energy gap and, consequently, in the color displayed by these two forms of indigo. This is also valid for the triplet energy which is significantly higher for DHI, when compared with indigo, with a difference between the two (keto-indigo and dehydroindigo) of 1.24 eV. This implies that, in marked contrast with indigo, DHI has a much smaller singlet−triplet energy splitting, leading to a very efficient $S_1 \rightsquigarrow T_1$ intersystem crossing process, and also a high efficiency of singlet oxygen sensitization, $S_\Delta = \phi_\Delta/\phi_T \sim 1$. Further studies (including theoretical calculations) on this oxidized species of indigo particularly on the relevance of rotational isomerism, a consequence of the single bond character of the central carbons of the molecule, in the properties of the lowest singlet and triplet excited states can potentially explain the amazing differences displayed by the three forms of this mythic molecule.

The analysis of the deactivation rate constants for DHI is complex because of the multiexponential nature of the decays, indicating that several species decay thus contributing to the overall deactivation of DHI in S_1. However, since we observe that the species contributing more to the total fluorescence (at longer wavelengths) is the longer component, with a value of 2 ns and a ϕ_T value of 0.156 in methanol (Table 1), we obtain a value for the intersystem crossing rate constant, $k_{ISC} = 7.8 \times 10^7\ s^{-1}$. This together with the 0.34 eV value of the S_1-T_1 energy splitting gives values typically close to those found for aromatic hydrocarbons,[43] providing convincing evidence that the triplet state of the oxidized form of indigo is, similarly to its neutral keto-indigo,[34] of π,π^* origin.

In toluene, S_1 is of n,π^* origin whereas T_1 (or the interacting triplet) is of π,π^* origin. In methanol S_1 is of π,π^* origin and T_1 is still of π,π^* origin. As a consequence of this and in full agreement with El-Sayed rules, the intersystem crossing process (as seen by the ϕ_T value) is more efficient in toluene ($\phi_T =$ 0.89, Table 1) than it is in methanol ($\phi_T = 0.189$, Table 1) since in the first case the coupling involves singlet and triplet states of different origin (n,π^* and π,π^*) and in the second case of identical (π,π^*) origin.[44−46]

Theoretical Calculations on the Electronic Structures of the S_0, S_1, and T_1 States of DHI. Within the framework of the density functional theory (DFT), the structures of the ground and excited states of DHI could be further accounted. The molecular geometries of DHI were optimized at the B3LYP/6-31G** level without imposing any symmetry constrains.

SCHEME 2: Schematic Presentation of the Kinetics in the Ground and First Excited Singlet State for DHI in Methanol and Glycerol

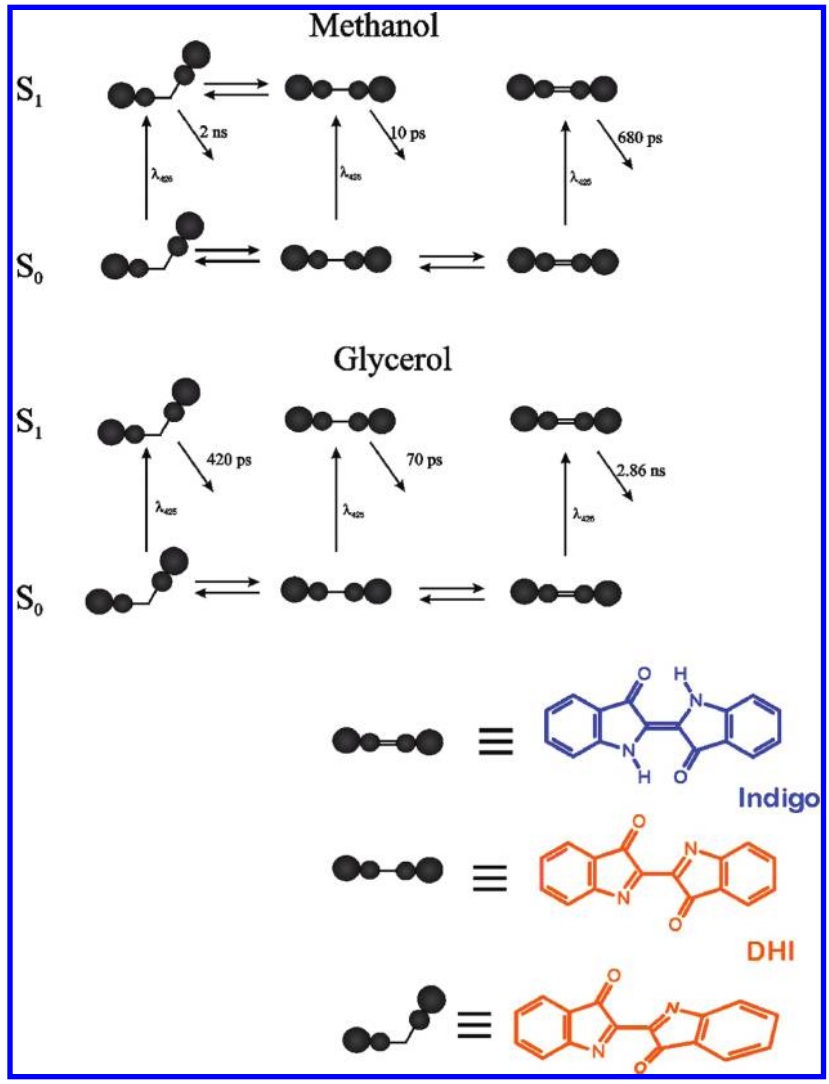

Different structures for the S_0, S_1, and T_1 electronic states, shown in Figure 7 through the bond distances in these three states, were obtained.

The energy difference between the HOMO and LUMO orbitals (vertical transition) gives a value of 3.01 eV which agrees well with the energy obtained for the, also vertical, transition (wavelength maxima) in methanol, 3.1 eV; see Table 1. However, and by comparison with the experimental S_0-T_1 energy gap of 2.28 eV, Scheme 3, theory seems to fail since now the energy gap is predicted to be 1.13 eV which is less than a half of the experimental value and much closer to that found for the triplet state of indigo.[34,41] Further studies on the (theoretical) location of the triplet, namely using a different basis set, should provide a more accurate location of the (predicted) triplet state of DHI.

Figure 8 shows the ground-state-optimized geometries for DHI together with the molecular contours of the relevant molecular orbitals (HOMO−1, HOMO, LUMO, LUMO+1). From these DFT calculations, the HOMO orbital shows a clear nonbonding character imparted by the nonbonding orbitals in the carbonyl oxygen. In contrast, the LUMO orbital shows a π-antibonding character; this results in a HOMO → LUMO n,π^* transition which is in agreement with the experimental data found in toluene (with residual water). However, like experimentally found in methanol, the lowest lying excited state is of π,π^* origin. In Figure 8, the molecular contours in the HOMO−1 are localized along the π-orbitals of the carbon atoms of the six- and five-member rings. This is compatible with a π,π^* transition (involving the HOMO−1 and the LUMO and LUMO+1 orbitals) which corroborates the finding that in methanol the lowest lying transition is of π,π^* origin.

It is now worth returning to the different geometries displayed by the S_0, S_1, and T_1 states. In the case of S_0, the predicted (more stable) geometry shows a deviation from planarity of 19.72° (dihedral angle between the N−C−C−N bonds) whereas in S_1 and T_1 the more stable geometry is now close to planarity.

The bond length in Figure 7 show that contrary to what has been described with indigo, where DFT calculations show that there is basically no change in the bond length of the six-member rings (of indigo),[41] in the case of DHI there is a difference between the bond length values of the more peripheral bonds of these six-member rings and those more closed to the five-member rings, indicating less delocalization to the outer bonds. As with indigo,[41] the antibonding character of the C═O bond is increased in DHI upon going from S_0 to S_1, which is mirrored by a lengthening of the bond (from 1.210 to 1.234 Å). However, the most significant and interesting change in bond length occurs in the central CC bond where the bond distances decrease in going from S_0 to T_1 (0.075 Å) indicating a gain of the double bond character in T_1. The change in this central CC bond length

SCHEME 3: Diagrams Showing for Indigo (left) and DHI in Methanol (right) the Different Values for the Quantum Yields of Excited State Deactivation and Energies (in eV) of the Lowest Lying Singlet and Triplet Excited States

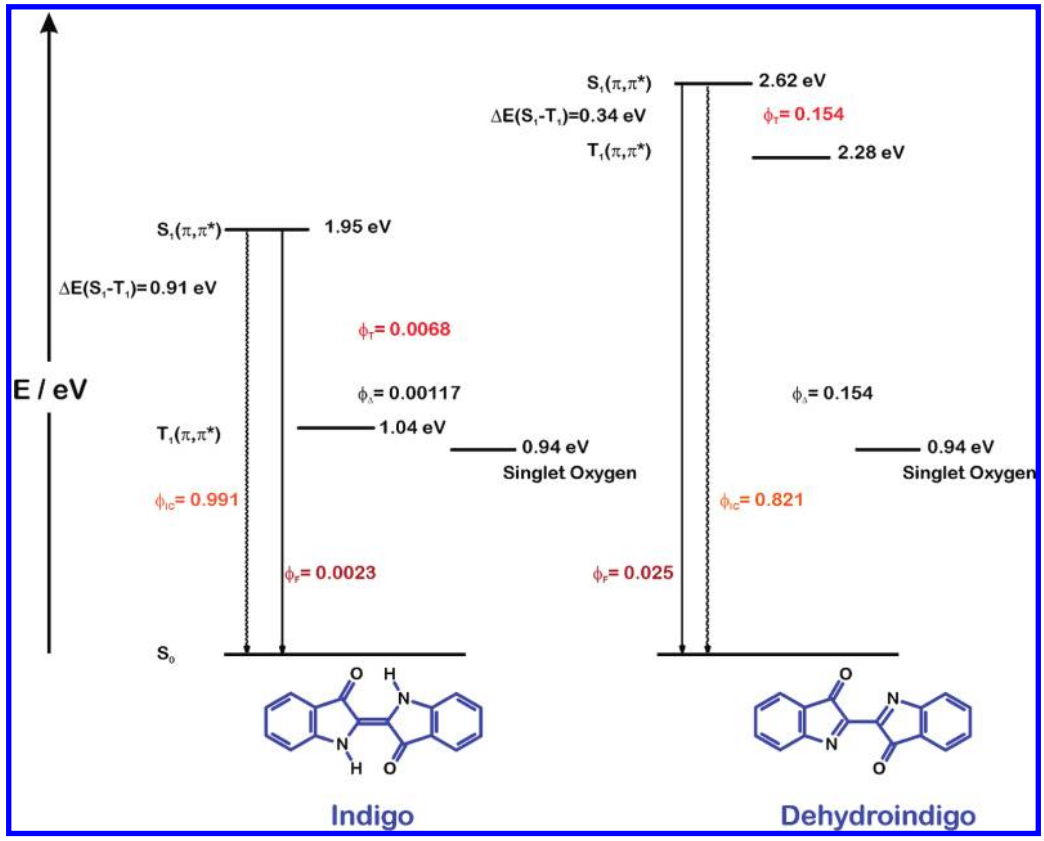

upon going from S_0 to S_1 is insignificant (0.006 Å) indicating that the single bond character of this bond allows the existence of different conformers in both the ground and singlet excited state, as discussed above in the time-resolved fluorescence section.

Again with indigo, others have found that, with similar DFT calculations, the $S_0 \rightarrow T_1$ transition causes a significant increase in the length of the CC central bond (from 1.361 to 1.423 Å) resulting in the change of this central carbon−carbon bond from a double (S_0) to a single bond (T_1) character.[41] This seems to be in line with the absence of phosphorescence[22] in indigo, not only because of the small S_0-T_1 energy gap, 1.04 ± 0.10 eV[34] (which from the golden rule for the radiationless transitions would favor this channel of deactivation), but also because of the single bond character of the carbon−carbon bond in indigo, allowing a loose bolt effect of this central bond (acting as a stretching or twisting vibration mode promoter of an efficient radiationless transition), which would promote the coupling between the T_1 and S_0 nonradiative modes[46] turning on the $T_1 \rightsquigarrow S_0$ into a very efficient process.

In contrast with indigo is DHI, where theory predicts the opposite situation, Figure 7; i.e., in the triplet state of this oxidized form of indigo the central carbon−carbon bond has now a double bond character. This would explain the observation of phosphorescence since the now more rigid (absence of rotation around the central carbon−carbon bond) together with the high S_0-T_1 energy gap value, 2.28 eV (Scheme 3), would decrease the coupling between the nonradiative modes of T_1 and S_0, favoring the radiative channel.[46]

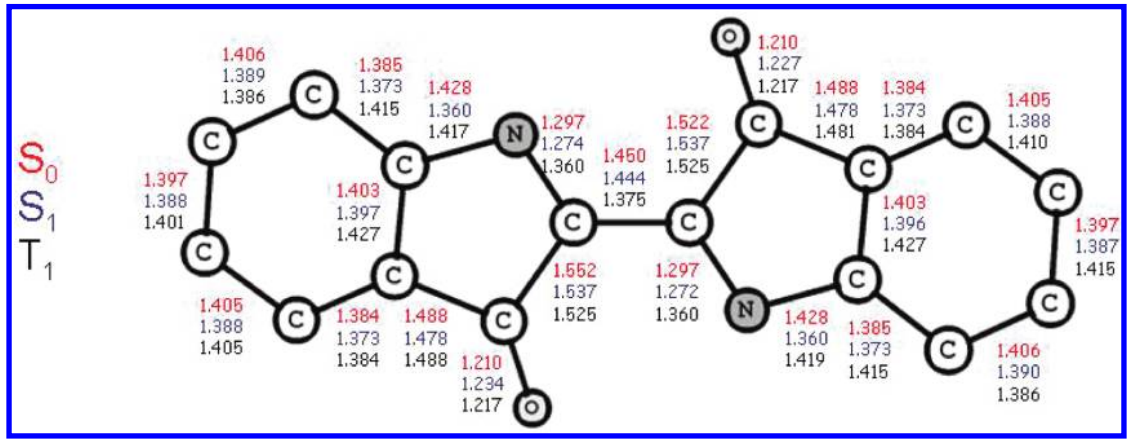

Figure 7. Bond length (in Å) calculated for DHI using DFT calculations (B3LYP 6-31G** level) for the electronic ground (S_0) and first singlet (S_1) and triplet excited (T_1) states.

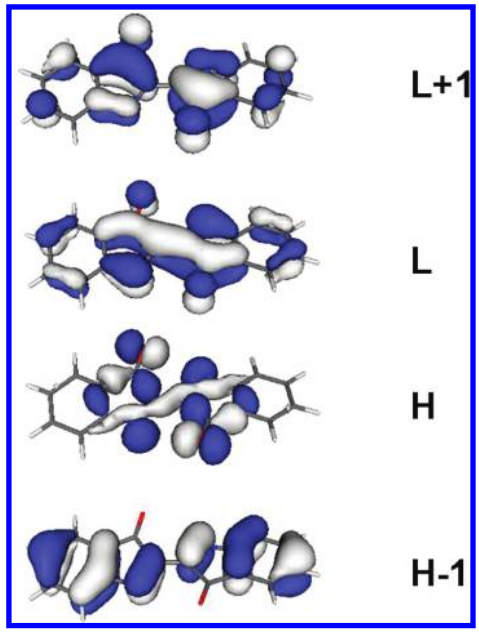

Figure 8. B3LYP 6-31G** optimized ground-state molecular structures for the HOMO (H), HOMO−1 (H-1), LUMO (L), and LUMO+1 (L+1) molecular orbital contours of DHI.

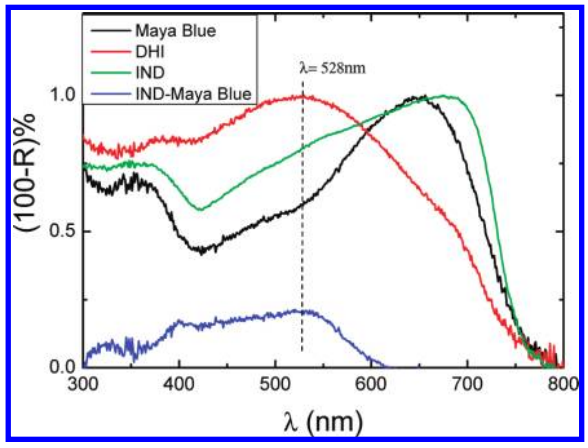

Figure 9. Solid-state spectra (diffuse reflection) of Maya Blue, dehydroindigo (DHI), and indigo (IND) in the 300−800 nm range, together with the difference spectra between indigo and Maya Blue (IND−Maya Blue) in the 300−650 nm range.

DHI and Maya Blue. The solid-state spectra (obtained by diffuse reflection) of indigo, DHI, and Maya Blue are shown in Figure 9 together with the spectra resulting from the subtraction of indigo to Maya Blue.

From these spectra several important observations could be drawn. First of all it is clear that the 558 nm absorption band maxima for DHI is, in the solid state, strongly red-shifted relative to the solution spectra (Figures 1 and 2 and Table 1). The same happens with indigo shifting from 600−620 nm (Table 1 and refs 22, 33, 47, and 48 and references therein) to 650 nm in the solid state and 680 nm in Maya Blue (Figure 9).

The wavelength maximum of indigo in Maya Blue suffers a blue shift when compared to indigo itself. Also worth noting is the observation that, in the solid state, indigo displays a much more broad visible absorption band than in solution,[22] which is clearly related to the stacking of the indigo molecules in the solid leading to aggregate absorption. Very interesting is also the observation that the spectra of indigo in Maya Blue is more sharp and close to that of indigo in solution (exception made to the difference in the wavelength maxima) clearly indicating the nature of the isolated molecules of indigo in the sepiolite channels of Maya Blue.

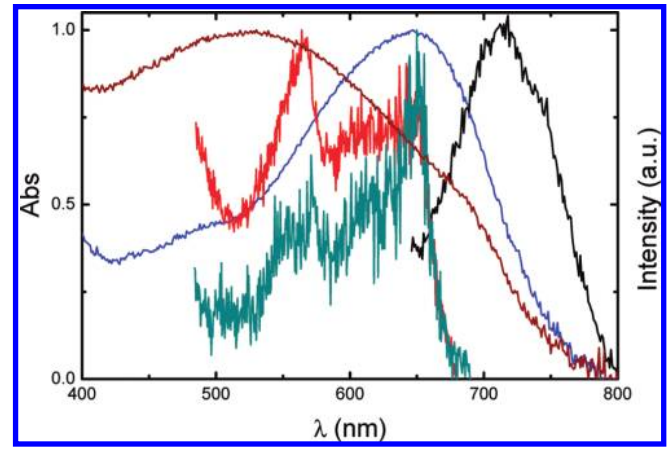

Figure 10. Solid-state absorption spectra for Maya Blue (blue trace) and DHI (brown trace) together with fluorescence emission spectra (black trace) and fluorescence excitation spectra collected with 7 days of difference (red trace, first; olive green trace, after) for Maya Blue. All spectra (absorption and fluorescence) are normalized to one.

The most interesting feature is, however, the observation that Maya Blue and DHI share a common band at ∼528 nm; see Figure 9. The spectral difference between indigo (in the solid) and Maya Blue leads to a band with maxima and shape very close to that of DHI (in the solid state), Figure 9, clearly suggesting the presence of DHI in Maya Blue in agreement with other recently published studies.[3,4,6,13,16] Moreover, it is also worth stressing that the location of the absorption band maxima of DHI in Maya Blue with that of DHI in solution (∼480 nm)[16] should be revised in light of the present data.

An additional relevant piece of information, relative to the contribution of DHI to Maya Blue, is obtained from the fluorescence excitation spectra of Maya Blue collected with a difference of 7 days. As can be seen from Figure 10, the fluorescence excitation spectra of Maya Blue presents two bands: one at 650 nm, matching with that observed in the solid-state spectra of indigo in Maya Blue, together with an additional at 550 nm, close to that found for DHI in the solid state (∼528 nm). It is interesting to note that the excitation spectra are more sharp than the solid-state absorption suggesting, once again, that fluorescence mirrors the behavior of individual molecules found inside (or at the surface) the channels of the clay. A last but not least important observation in the spectra is that when collected with an interval of 7 days, the 550 nm band (DHI) contribution decreases relative to the 650 nm (indigo) band. Although further and detailed studies (which are currently in progress including time-resolved experiments on Maya Blue) are needed, this clearly suggests that, albeit not significant, there is, with time, a conversion (most likely inside the clay channels) of DHI into indigo.

Conclusions

In aqueous solution or in protic solvents, DHI has the tendency to extract hydrogen from the media giving rise to the neutral blue indigo. Depending on the solvent, dehydroindigo displays different spectral and photophysical properties.

The photophysics of DHI is remarkably different from the neutral indigo keto (blue) form and also from the reduced indigo leuco form. In contrast with the behavior found for indigo, the main deactivation pathway of the excited state in DHI is the $S_1 \rightsquigarrow T_1$ intersystem crossing with reduced contributions from

fluorescence and $S_1 \rightsquigarrow S_0$ internal conversion. However, this was found to be solvent dependent. This gives further support for the fast deactivation, via the radiationless internal conversion channel, of indigo which must be operative in this neutral form through intramolecular proton transfer from the N—H to the C═O groups.[33,35,49]

Time-resolved fluorescence decays reveal a fit to a triple exponential decay law, which is compatible with the presence of rotational isomerization.

The electronic structure of the ground and first excited singlet and triplet electronic states was interpreted with the help of DFT calculations. These showed that, in contrast with indigo, where the central carbon−carbon bond has a double bond character in the ground state and a single bond character in the triplet state, in DHI the opposite situation was found. This, together with the fact that the T_1 state was experimentally found to be located at 2.28 eV (in contrast to the 1.04 eV value for indigo), suggests an explanation for the observed efficient radiative deactivation of the triplet state.

The contribution of DHI to the color of the pigment Maya Blue was further investigated by optical and fluorescence spectroscopy in the solid state. The comparison between the spectra of DHI, indigo and Maya Blue in the solid state suggests that DHI is present, together with indigo, in the spectra (and therefore the color) of Maya Blue. In addition, the spectrum of DHI in the solid state was found to be significantly red-shifted when compared to the value in solution.

The results here provided for DHI constitute additional elements aimed at understanding the rich palette of colors displayed by the ancient blue of the Maya civilization, in view of the demonstrated presence of this form of indigo in the formation and constitution of Maya Blue.

Acknowledgment. We are grateful to POCI (through projects PTDC/EAT/65445/2006 and PTDC/QUI-QUI/099388/2008), FCT, and FEDER for further funding. R.R. acknowledges FCT for a PhD grant (SFRH/BD/38882/2007). J.S.S.M. acknowledges Professor A. Pais, Dr. P. Abreu, and Dr. João Pina for help with the interpretation of the DFT calculations.

References and Notes

(1) Balfour-Paul, J. *Indigo*; British Museum Press: London, 2000.
(2) Sousa, M. M.; Miguel, C.; Rodrigues, I.; Parola, A. J.; Pina, J.; Seixas de Melo, J. S.; Melo, M. J. *Photochem. Photobiol. Sci.* **2008**, *7*, 1353.
(3) Domenech, A.; Domenech-Carbo, M. T.; Pascual, M. *J. Phys. Chem. C* **2007**, *111*, 4585.
(4) Domenech, A.; Domenech-Carbo, M. T.; Pascual, M. *J. Phys. Chem. B* **2006**, *110*, 6027.
(5) Domenech, A.; Domenech-Carbo, M. T.; Pascual, M. *J. Solid State Electrochem.* **2007**, *11*, 1335.
(6) Tilocca, A.; Fois, E. *J. Phys. Chem. C* **2009**, *113*, 8683.
(7) Vanolphe, H. *Science* **1966**, *154*, 645.
(8) del Rio, M. S.; Picquart, M.; Haro-Poniatowski, E.; Van Elslande, E.; Uc, V. H. *J. Raman Spectrosc.* **2006**, *37*, 1046.
(9) Manciu, F. S.; Reza, L.; Polette, L. A.; Torres, B.; Chianelli, R. R. *J. Raman Spectrosc.* **2007**, *38*, 1193.
(10) Giustetto, R.; Levy, D.; Chiari, G. *Eur. J. Mineral.* **2006**, *18*, 629.
(11) Berke, H. *Chem. Soc. Rev.* **2007**, *36*, 15.
(12) Polette-Niewold, L. A.; Manciu, F. S.; Torres, B.; Alvarado, M.; Chianelli, R. R. *J. Inorg. Biochem.* **2007**, *101*, 1958.
(13) del Rio, M. S.; Boccaleri, E.; Milanesio, M.; Croce, G.; van Beek, W.; Tsiantos, C.; Chyssikos, G. D.; Gionis, V.; Kacandes, G. H.; Suarez, M.; Garcia-Romero, E. *J. Mater. Sci.* **2009**, *44*, 5524.
(14) Chiari, G.; Giustetto, R.; Druzik, J.; Doehne, E.; Ricchiardi, G. *Appl. Phys. A: Mater. Sci. Process.* **2008**, *90*, 3.
(15) Museum, F. Centuries-old Maya Blue Mystery Finally Solved. In *ScienceDaily* 2008, February 28.
(16) Domenech, A.; Domenech-Carbo, M. T.; del Rio, M. S.; Goberna, S.; Lima, E. *J. Phys. Chem. C* **2009**, *113*, 12118.
(17) Kalb, L. *Ber. Dtsch. Chem. Ges.* **1909**, *42*, 3642.
(18) Klessinger, M.; Luettke, W. *Tetrahedron* **1963**, *19* (Suppl. 2), 315.
(19) Lütke, W.; Klessinger, M. *Chem. Ber.* **1964**, *97*, 2342.
(20) Murov, S.; Carmichael, I.; Hug, G. L. *Handbook of Photochemistry*; Marcel Dekker, Inc.: New York, 1993.
(21) Becker, R. S.; Seixas de Melo, J.; Maçanita, A. L.; Elisei, F. *J. Phys. Chem.* **1996**, *100*, 18683.
(22) Seixas de Melo, J.; Moura, A. P.; Melo, M. J. *J. Phys. Chem. A.* **2004**, *108*, 6975.
(23) Martinez, C. G.; Neumer, A.; Marti, C.; Nonell, S.; Braun, A. M.; Oliveros, E. *Helv. Chim. Acta* **2003**, *86*, 384.
(24) Pina, J.; Seixas de Melo, J.; Burrows, H. D.; Maçanita, A. L.; Galbrecht, F.; Bunnagel, T.; Scherf, U. *Macromolecules* **2009**, *42*, 1710.
(25) Striker, G.; Subramaniam, V.; Seidel, C. A. M.; Volkmer, A. *J. Phys. Chem. B* **1999**, *103*, 8612.
(26) Seixas de Melo, J.; Silva, L. M.; Kuroda, M. *J. Chem. Phys.* **2001**, *115*, 5625.
(27) Bensasson, R. V.; Land, E. J.; Truscott, T. G. *Excited States and Free Radicals in Biology and Medicine. Contributions from Flash Photolysis and Pulse Radiolysis*; Oxford University Press: Oxford, 1993.
(28) Frisch, M. J.; Trucks, G. W.; Schlegel, H. B.; Scuseria, G. E.; Robb, M. A.; Cheeseman, J. R. ; Montgomery, J. A., Jr.; Vreven, T.; Kudin, K. N.; Burant, J. C.; Millam, J. M.; Iyengar, S. S.; Tomasi, J.; Barone, V.; Mennucci, B.; Cossi, M.; Scalmani, G.; Rega, N.; Petersson, G. A.; Nakatsuji, H.; Hada, M.; Ehara, M.; Toyota, K.; Fukuda, R.; Hasegawa, J.; Ishida, M.; Nakajima, T.; Honda, Y.; Kitao, O.; Nakai, H.; Klene, M.; Li, X.; Knox, J. E.; Hratchian, H. P.; Cross, J. B.; Bakken, V.; Adamo, C.; Jaramillo, J.; Gomperts, R.; Stratmann, R. E.; Yazyev, O.; Austin, A. J.; Cammi, R.; Pomelli, C.; Ochterski, J. W.; Ayala, P. Y.; Morokuma, K.; Voth, G. A.; Salvador, P.; Dannenberg, J. J.; Zakrzewski, V. G.; Dapprich, S.; Daniels, A. D.; Strain, M. C.; Farkas, O.; Malick, D. K.; Rabuck, A. D.; Raghavachari, K.; Foresman, J. B.; Ortiz, J. V.; Cui, Q.; Baboul, A. G.; Clifford, S.; Cioslowski, J.; Stefanov, B. B.; Liu, G.; Liashenko, A.; Piskorz, P.; Komaromi, I.; Martin, R. L.; Fox, D. J.; Keith, T.; Al.Laham, M. A.; Peng, C. Y.; Nanayakkara, A.; Challacombe, M.; Gill, P. M. W.; Johnson, B.; Chen, W.; Wong, M. W.; Gonzalez, C.; Pople, J. A. *Gaussian 03, Revision C.02*; Gaussian, Inc.: Wallingford, CT, 2004.
(29) Becke, A. D. *J. Chem. Phys.* **1993**, *98*, 1372.
(30) Francl, M. M.; Pietro, W. J.; Hehre, W. J.; Binkley, J. S.; Gordon, M. S.; Defrees, D. J.; Pople, J. A. *J. Chem. Phys.* **1982**, *77*, 3654.
(31) Portmann, S.; Luthi, H. P. *Chimia* **2000**, *54*, 766.
(32) Valeur, B. *Molecular Fluorescence: Principles and Applications*; Wiley-VCH: Weinheim, 2002.
(33) Seixas de Melo, J. S.; Rondão, R.; Burrows, H. D.; Melo, M. J.; Navaratnam, S.; Edge, R.; Voss, G. *ChemPhysChem* **2006**, *7*, 2303.
(34) Seixas de Melo, J. S.; Serpa, C.; Burrows, H. D.; Arnaut, L. G. *Angew. Chem., Int. Ed.* **2007**, *46*, 2094.
(35) Seixas de Melo, J.; Rondão, R.; Burrows, H. D.; Melo, M. J.; Navaratnam, S.; Edge, R.; Voss, G. *J. Phys. Chem. A.* **2006**, *110*, 13653.
(36) Wyman, G. M.; Zenhause, A. F. *J. Org. Chem.* **1965**, *30*, 2348.
(37) Abe, J.; Nagasawa, Y.; Takahashi, H. *J. Chem. Phys.* **1989**, *91*, 3431.
(38) Pina, J.; Seixas de Melo, J. *Phys. Chem. Chem. Phys.* **2009**, *11*, 8706.
(39) Gorman, A. A.; Lovering, G.; Rodgers, M. A. J. *J. Am. Chem. Soc.* **1978**, *100*, 4527.
(40) Haucke, G.; Seidel, B.; Graness, A. *J. Photochem.* **1987**, *37*, 139.
(41) Ngan, V. T.; Gopakumar, G.; Hue, T. T.; Nguyen, M. T. *Chem. Phys. Lett.* **2007**, *449*, 11.
(42) Klessinger, M. *Angew. Chem., Int. Ed. Engl.* **1980**, *19*, 908.
(43) Malkin, J. *Photophysical and Photochemical Properties of Aromatic Compounds*; CRC Press: Boca Raton, FL, 1992.
(44) El- Sayed, M. A. *Acc. Chem. Res.* **1968**, *1*, 8.
(45) Becker, R. S. *Theory and Interpretation of Fluorescence and Phosphorescence*; Wiley-Interscience: New York, 1969.
(46) Turro, N. *Modern Molecular Photochemistry*; University Science Books: Sausalito, CA, 1991.
(47) Zollinger, H. *Color Chemistry. Synthesis, Properties, and Applications of Organic Dyes and Pigments*, 3rd ed.; Verlag Helvetica Chimica Acta & Wiley-VCH: Zürich, 2003.
(48) Jacquemin, D.; Preat, J.; Wathelet, V.; Perpete, E. A. *J. Chem. Phys.* **2006**, *124*, 074104.
(49) Iwakura, I.; Yabushita, A.; Kobayashi, T. *Chem. Lett.* **2009**, *38*, 1020.

JP907718K